Acceptor-like deep level defects in ion-implanted ZnO

L. Vines, , J. Wong-Leung, , C. Jagadish, , V. Quemener, , E. V. Monakhov, and , and B. G. Svensson

Citation: Appl. Phys. Lett. **100**, 212106 (2012); doi: 10.1063/1.4720514
View online: http://dx.doi.org/10.1063/1.4720514
View Table of Contents: http://aip.scitation.org/toc/apl/100/21
Published by the American Institute of Physics

Acceptor-like deep level defects in ion-implanted ZnO

L. Vines,[1,a)] J. Wong-Leung,[2] C. Jagadish,[2] V. Quemener,[1] E. V. Monakhov,[1] and B. G. Svensson[1]
[1]*Department of Physics/Centre for Materials Science and Nanotechnology, University of Oslo, P.O. Box 1048 Blindern, N-0316 Oslo, Norway*
[2]*Department of Electronic Materials Engineering, Research School of Physics and Engineering, The Australian National University, Canberra ACT 0200, Australia*

(Received 13 March 2012; accepted 8 May 2012; published online 22 May 2012)

N-type ZnO samples have been implanted with MeV Zn^+ ions at room temperature to doses between 1×10^8 and 2×10^{10}cm^{-2}, and the defect evolution has been studied by capacitance-voltage and deep level transient spectroscopy measurements. The results show a dose dependent compensation by acceptor-like defects along the implantation depth profile, and at least four ion-induced deep-level defects arise, where two levels with energy positions of 1.06 and 1.2 eV below the conduction band increase linearly with ion dose and are attributed to intrinsic defects. Moreover, a re-distribution of defects as a function of depth is observed already at temperatures below 400 K. © *2012 American Institute of Physics*. [http://dx.doi.org/10.1063/1.4720514]

Zinc oxide (ZnO) is a wide band gap semiconductor ($E_g \sim 3.4$ eV) that has received considerable attention during the past few years due to its potential applications in light emitting devices and photovoltaics. However, the technological advances of ZnO have been hindered by the difficulty in controlling and understanding the electrical behavior of intrinsic and impurity related defects. In particular, controlling charge carrier concentration profiles by ion implantation remains a major challenge for ZnO based devices. This includes both dopant activation in the desired atomic configuration and control of ion induced damage.

Studying irradiated or implanted samples is indispensable for the understanding of electrically active defects, both intrinsic and impurity related ones, where deep level transient spectroscopy (DLTS) is one of the most sensitive techniques. Intrinsic defects are of particular importance in ZnO, since many of those are expected to be electrically active and play an important role for the "native" n-type conduction and the difficulty in achieving p-type doping. However, only a few irradiation studies of ZnO using DLTS have been reported so far;[1–4] in fact, most of the irradiation studies have been carried out using light projectiles such as electrons, protons, and helium ions, mainly focusing on defects detectable below 300K. However, recent advances in the quality of Schottky contacts have made it possible to extend the DLTS temperature range up to 600 K and to probe deep into the band gap.[5,6]

Here, we report on 3 and 6 MeV Zn^+ implantation into ZnO in the low dose regime and several defect levels are observed above 300 K. Moreover, a re-distribution of defects occurs below 400 K, indicating a high mobility, consistent with an efficient dynamic annealing but possibly also with formation of large and more stable defect clusters.

Two wafers of hydrothermally grown ZnO (HT-ZnO) from Tokyo Denpa, labelled W1 and W2, were cut into four 5×5 mm samples. The samples were cleaned in acetone and ethanol and treated for 1 min in boiling H_2O_2 before 100 nm thick Pd Schottky contacts were deposited using e-beam evaporation. The Schottky contacts showed a rectification of the current by 2-4 orders of magnitude between forward and reverse bias. The samples were then implanted at room temperature using 3 MeV Zn^{3+} ions for the W1 samples and 6 MeV Zn^{6+} ions for the W2 samples, and with doses ranging from 1×10^8 to 2×10^{10}cm^{-2}. One sample of each wafer was left as reference (non-implanted) and no influence of the implantation dose on the rectifying behavior of the Schottky contacts was found. The projected range (R_p) of the Zn ions was $\sim 1.0\,\mu$m and $\sim 1.9\,\mu$m for the 3 and 6 MeV implantations, respectively, as estimated by simulations using the SRIM code.[7] As an example, the peak Zn concentration for the 6 MeV implantation and a dose of 5×10^8 cm^{-2} is $\sim 1.5 \times 10^{13}$cm^{-3}. After implantation, the samples were stored in a freezer (−20 °C) until measured. DLTS was carried out while scanning up in temperature using a refined version of a setup described in Ref. 8. A reverse bias of −3 V was used with a filling pulse of +3 V and 5 ms duration.

Figure 1(a) shows the charge carrier concentration (N_d) versus depth extracted from capacitance-voltage (CV) measurements at 300 K for the W1 samples implanted with doses between 8×10^8 and 2×10^{10}cm^{-2}; scan 1 is the first one after implantation. Before implantation, $N_d \sim 1.2 \times 10^{15}$cm^{-3} and is uniform as a function of depth. The sample implanted with the low dose (8×10^8cm^{-2}) shows only minor changes in the charge carrier distribution (scan 1), but a significant redistribution takes place for the medium (5×10^9 cm^{-2}) and high (2×10^{10}cm^{-2}) dose samples. For the highest dose, a strongly reduced charge carrier concentration occurs around R_p followed by a pronounced increase below R_p. This increase is not real and attributed to an anomaly occuring when profiling nonuniform distributions of deep acceptor-like centers.[9] Indeed, Fig. 1(b) shows the carrier concentration, after DLTS scan 2, at different temperatures using a probing frequency of 1 MHz and sweep frequency of 5 Hz; in accordance with Kimerling,[9] the anomalous overshoot below R_p occurs only at certain temperatures, i.e., when the emission rate from the deep acceptor is intermediate to the sweep rate and the probing rate.

a)Lasse.Vines@fys.uio.no.

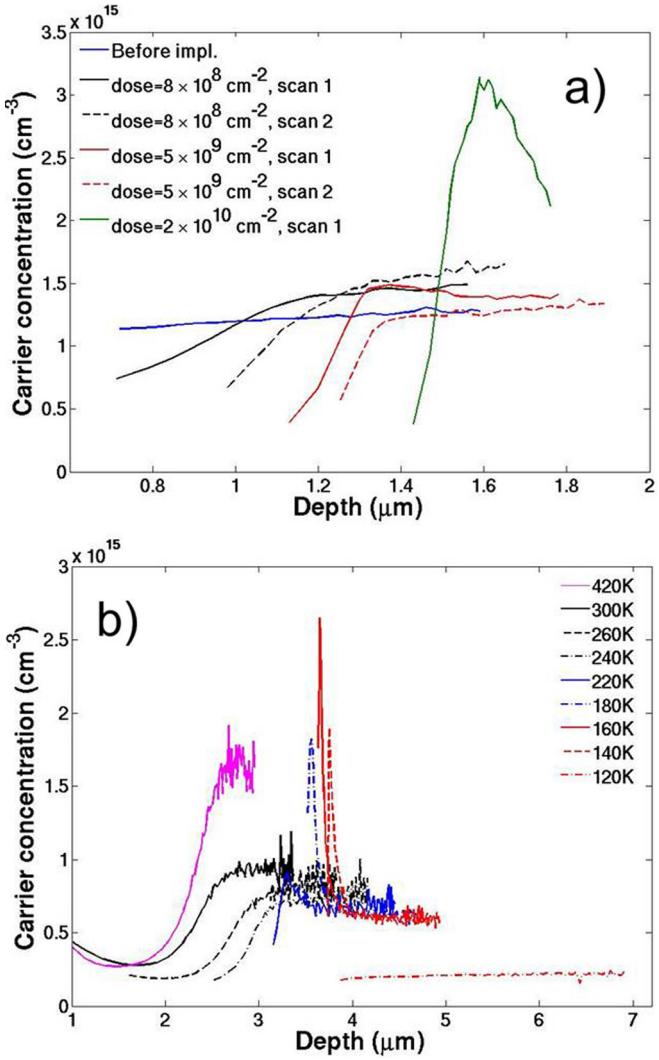

FIG. 1. Carrier concentration versus depth profiles for (a) W1-samples implanted by 3 MeV Zn ions to different doses and (b) W2-sample implanted with 6 MeV Zn ions to a dose of $1.2 \times 10^9 \text{cm}^{-2}$ and analysed at different temperatures after scan 2 (probing frequency = 1 MHz).

Further, Fig. 1(a) reveals a considerable re-distribution or generation of defects between the as-implanted (scan 1) and ~410 K annealed profiles (scan 2), where N_d in the near-surface region decreases after annealing and with increasing dose. For the high dose sample ($2 \times 10^{10}\,\text{cm}^{-2}$), a complete freeze-out of N_d occurs in scan 2. Scan 3 remained similar to scan 2, and for clarity, data are not included in the figure. Moreover, the as-grown samples did not show a reduced carrier concentration in the near surface region or a change in the profile after successive DLTS scans (not shown). Thus, an acceptor activation or donor removal occur in the implanted samples during the first scan, demonstrating that migration or defect reactions take place below 420 K. For instance, theory predicts that zinc interstitials (Zn_I) have a migration barrier of ~0.6 eV,[10] indicating that they are mobile around room temperature and can readily migrate towards the bulk or the surface during the first scan.

Another species with high mobility, and abundant in ZnO, is hydrogen (H),[11,12] which may act as a donor and/or passivant of acceptors. Interstitial H is usually regarded to have a migration energy of ~0.8 eV,[13–15] i.e., sufficiently low to enable migration lengths in excess of 100 nm during scan 1. The CV-profiles show an evolution of deep acceptor centers after scan 1 implying that donor-like defects like Zn_I and H_O/H_I do not play a direct role. However, activation of H-passivated acceptors with states in the upper part of E_g cannot be excluded, although H is not expected to leave the damaged region around R_p but rather form more stable complexes.[16] Further, the reduction in N_d at R_p is at least a factor of 5 higher than the concentration of implanted Zn showing that ion-induced defects are involved in the evolution/activation of deep acceptors, possibly in combination with an abundant impurity, like H.

Figure 2 shows DLTS spectra for the W1 and W2 samples taken immediately after implantation (scan 1), except for the sample implanted with a dose of $8 \times 10^8\,\text{cm}^{-2}$ which received an annealing (>350 K) before the measurement. At least four levels are present, labeled E3-E6. The spectrum for the highest dose sample ($2 \times 10^{10}\text{cm}^{-2}$) is omitted due to the strong carrier compensation, as evident from Fig. 1, but it follows the same trend as the other samples. A pronounced peak of the well-known level around $E_c - 0.3$ eV (E_c denotes the conduction band edge), normally labeled E3,[17] is found in the as-grown samples, and the strength varies by more than a factor of two between the two wafers. However, the amplitude of E3 does not change significantly after implantation. The level labeled E4, with a position of $E_c - 0.57$ eV, has also been reported previously[17] and tentatively assigned to the oxygen vacancy (V_O).[18] Interestingly, the concentration of E4 is low in the present samples, in contrast to that reported by other authors after electron and light ion irradiation.[1,3] This casts doubts on the identification of E4 as V_O, since V_O is a primary defect and anticipated to increase in concentration with ion dose.

Less is known about the level labeled E5, with an energy position of ~1.06 eV below E_c, since DLTS results above room temperature are scarce in the literature, primarily because of poor quality Schottky contacts.[5] In most of the as-implanted samples, the E5 peak is accompanied by a shoulder on the low temperature tail, labeled E5b, and with a position of $\sim E_c - 0.90$ eV. Both E5 and E5b exhibit a strong dose dependence, where the concentration of E5 in samples implanted with 1.2×10^9 ions/cm^2, or higher, exceeds the

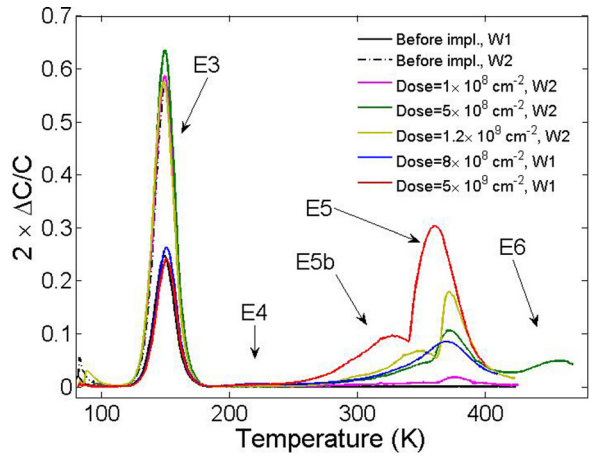

FIG. 2. DLTS signal ($2 \times \Delta C/C$) for samples before and after implantation with 3 MeV (W1) and 6 MeV (W2) Zn to doses from 1×10^8 to $5 \times 10^9\,\text{cm}^{-2}$.

maximum limit ($\lesssim$10% of N_d) for a quantitative DLTS analysis. As a result, charge carrier freeze out by E5 becomes substantial and the peak position shifts towards lower temperatures in the highest dose sample ($5 \times 10^9\,\mathrm{cm}^{-2}$).[19] The asymmetric shape of the E5 peak, with a sharp rise on the low temperature side, should be noticed but further investigations are needed to clarify the origin of this behavior.

An even deeper level, E6, exists in the $5 \times 10^8\,\mathrm{cm}^{-2}$ sample where the upper temperature of the DLTS scan was extended to 460 K. The extracted energy position is $\sim E_c - 1.2$ eV, based on data for 3 rate windows covering the E6 peak within 460 K. Interestingly, two levels similar to E5 and E6, appearing in the same temperature range and with similar energy positions, have been observed in samples exposed to mechanical polishing.[5] This suggests an intrinsic origin of E5 and E6 and their general importance in processing of ZnO. In Ref. 5, they were tentatively assigned to vacancies or clusters thereof.

Figure 3 shows DLTS spectra of the W2 sample before and after implantation with 6 MeV Zn ions to a dose of $5 \times 10^8\,\mathrm{cm}^{-2}$. The inset in Fig. 3 displays the corresponding steady-state capacitance versus temperature. Several DLTS scans subsequent to scan 2 were also carried out but they yielded similar results as those of scan 2. Fig. 3 reveals a change in both concentration and peak position of E5, E5b, and E6 between the different scans. E5b appears to be highly unstable above ~400 K and disappears. E5 is reduced by $\sim 50\%$ and shifts towards higher temperatures, while E6 exhibits an increase of similar magnitude as the loss of E5. The reduction in reverse bias capacitance revealed by the inset of Fig. 3 complies with the results in Fig. 1, indicating activation/evolution of deep acceptors after the implant. Moreover, the temperature dependence of the electron emission rates from E5 and E5b deduced from scan 1 do not follow a strict Arrhenius behavior, suggesting that multiple levels may be present. However, for the subsequent DLTS scan (scan 2), an Arrhenius behavior is obeyed, and the estimated energy level positions stated above are taken from scan 2.

The strong generation of E5 (and E6) as a function of ion dose unveiled by Fig. 2 is striking, and the increase in amplitude exhibits a close to linear dose dependence. However, for a fully quantitative analysis, profiling measurements are required. Figure 4 illustrates such profiles of E3, E5, and E6 for the samples implanted with 5×10^8 and 1.2×10^9 ions/cm^2, while the amplitude of E4 is too low for reliable measurements. E3 displays an increasing concentration towards the bulk, and no dependence on ion dose is revealed. These results are fully consistent with the DLTS amplitudes of E3 in Figs. 2 and 3 and also with previous studies in the literature,[2,3,17] indicating that irradiation has a weak (if any) effect on the strength of E3. The strong E3 signal prior to implantation limits the accuracy of the extracted generation rate, but it is at least one order of magnitude lower than that of E5 and close to zero (within the experimental accuracy).

In contrast to E3, both E5 and E6 show a clear peak in the concentration around R_p (Fig. 4) and they are evidently implantation induced. From SRIM simulations,[7] and assuming a displacement threshold energy of 30 and 52 eV for Zn and O atoms, respectively,[20] the total peak vacancy generation is found to be 1.2 vacancies/ion/Å. For E6, the generation rate is found to be 9×10^{-4} centers per vacancy, which is more than one order of magnitude lower than the corresponding rate of the vacancy-oxygen pair and the divacancy center in Si.[21] Hence, one may argue that E6 arises from a complex rather than a primary (low-order) defect; on the other hand, ZnO is well known to exhibit pronounced dynamic annealing,[22] and a primary defect cannot be excluded. The concentration of E6 reaches a maximum close to R_p, with a rapid reduction towards the surface. Interestingly, the decrease towards the surface is sharper than that of the vacancy profile, as estimated by SRIM, and resembles more the implantation profile. In implanted layers, it is well established that the region deeper than R_p is interstitial rich, while the more shallow region is vacancy rich, see for example Ref. 23. Thus, it may be speculated that E6 is related to interstitials (Zn_I and/or O_I) rather than to vacancies (V_{Zn}, V_O).

In contrast, E5 has a clear surface tail, possibly suggesting a vacancy related center, in agreement with Ref. 5 and positron annihilation studies.[24] The peak generation rate of E5 is similar to that of E6, i.e., $\sim 9 \times 10^{-4}$ centers/vacancy

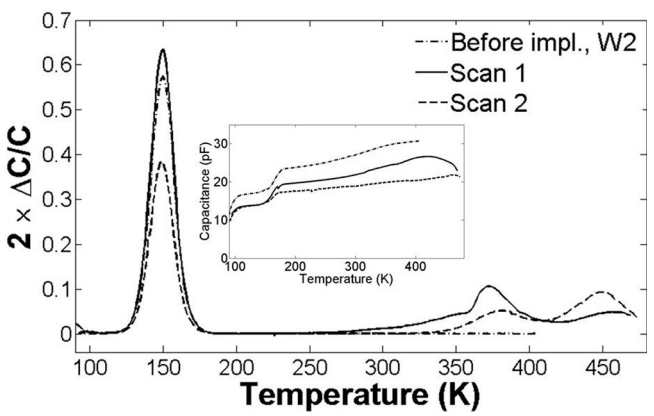

FIG. 3. DLTS signal ($2 \times \Delta C/C$) versus temperature for a W2 sample before and after implantation with 6 MeV Zn ions to a dose of $5 \times 10^8\,\mathrm{cm}^{-2}$, scans 1 and 2 are successive ones (up to 460 K) after the implantation.

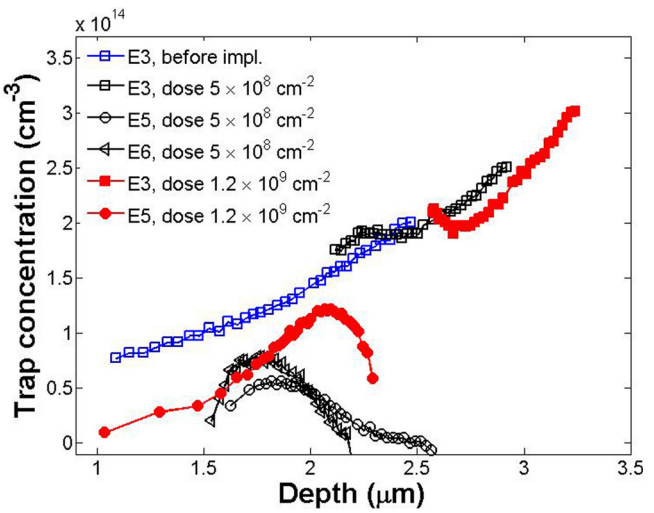

FIG. 4. Concentration versus depth profiles of E3, E5, and E6 for the W2 samples implanted with 6 MeV Zn ions to doses of 5×10^8 and $1.2 \times 10^9\,\mathrm{cm}^{-2}$, where the λ-effect have been taken into account.

and this value holds irrespective of ion dose confirming a linear dose dependence (Fig. 2). The linear dependence implies a dilute regime where the concentration of stable defects is not high enough to influence the trapping of migrating defects from neighbouring ion tracks.[21] Hence, E5 originates most likely from a primary defect of vacancy-type or a low-order vacancy cluster formed directly in single collision cascades.

In summary, n-type ZnO samples have been implanted with 3 and 6 MeV Zn^+ ions using doses between 8×10^8 and $2 \times 10^{10}\text{cm}^{-2}$, and the generation of electrically active defects has been studied by DLTS. C-V measurements show charge carrier compensation by deep acceptor-like traps evolving at depths $\lesssim R_p$ during modest post-implant annealing ($\sim$400 K). At least four implantation-induced deep-level defects arise, with energy positions of 0.57, 0.89, 1.06, and 1.2 eV below E_c. The two latter ones are scarcely reported for implanted/irradiated samples and both exhibit a generation rate of $\lesssim 1 \times 10^{-3}$ centers per vacancy (or interstitial) in the region around R_p. Based on their concentration-versus-depth profiles, it is argued that E5 is possibly vacancy-related while E6 is tentatively associated with interstitials.

This work was supported by the Norwegian Research Council through the Frienergi program and the Australian Research Council through the Discovery projects program.

[1]F. D. Auret, S. A. Goodman, M. Hayes, M. J. Legodi, H. A. van Laarhoven, and D. C. Look, Appl. Phys. Lett. **79**, 3074 (2001).
[2]M. Hayes, F. D. Auret, P. J. Janse van Rensburg, J. M. Nel, W. Wesch, and E. Wendler, Phys. Status Solidi B **244**, 1544 (2007).
[3]M. Hayes, F. D. Auret, P. J. Janse van Rensburg, J. M. Nel, W. Wesch, and E. Wendler, Nucl. Instrum. Methods Phys. Res. B **257**, 311 (2007).
[4]Z.-Q. Fang, B. Claflin, D. C. Look, and G. C. Farlow, J. Appl. Phys. **101**, 086106 (2007).
[5]V. Quemener, L. Vines, E. V. Monakhov, and B. G. Svensson, Appl. Phys. Lett. **99**, 112112 (2011).
[6]L. J Brillson and Y. Lu, J. Appl. Phys. **605**, 121301 (2011).
[7]J. F. Ziegler, J. P. Biersack, and U. Littmark, *The Stopping and Range of Ions in Solids* (Pergamon, New York, 1985).
[8]B. G. Svensson, K.-H. Rydén, and B. M. S. Lewerentz, J. Appl. Phys. **66**, 1699 (1989).
[9]L. C. Kimerling, J. Appl. Phys. **45**, 1839 (1974).
[10]A. Janotti and C. G. Van de Walle, Phys. Rev. B **75**, 165202 (2007).
[11]E. Mollwo, Z. Phys. **138**, 478 (1954).
[12]S. F. J. Cox, E. A. Davis, S. P. Cottrell, P. J. C. King, J. S. Lord, J. M. Gil, H. V. Alberto, R. C. Vilao, J. Piroto Duarte, N. Ayres de Campos, A. Weidinger, R. L. Lichti, and S. J. C. Irvine, Phys. Rev. Lett. **86**, 2601 (2001).
[13]D. G. Thomas and J. J. Lander, J. Chem. Phys. **25**, 1136 (1956).
[14]N. H. Nickel and K. Brendel, Phys. Rev. B **68**, 193303 (2003).
[15]K. M. Johansen, J. S. Christensen, E. V. Monakhov, A. Yu. Kuznetsov, and B. G. Svensson, Appl. Phys. Lett. **93**, 152109 (2008).
[16]E. V. Monakhov, J. S. Christensen, K. Maknys, B. G. Svensson, and A. Y. Kuznetsov, Appl. Phys. Lett. **87**, 191910 (2005).
[17]F. D. Auret, S. A. Goodman, M. J. Legodi, W. E. Meyer, and D. C. Look, Appl. Phys. Lett. **80**, 1340 (2002).
[18]T. Frank, G. Pensl, R. Tena-Zaera, J. Zúñiga-Pérez, C. Matńez-Tomás, V. Muñoz-Sanjosé, T. Ohshima, H. Itoh, D. Hofmann, D. Pfisterer, J. Sann, and B. Meyer, Appl. Phys A **88**, 141 (2007).
[19]E. V. Monakhov, J. Wong-Leung, A. Yu. Kuznetsov, C. Jagadish, and B. G. Svensson, Phys. Rev. B **65**, 245201 (2002).
[20]R. E. Williford, R. Devanathan, and W. J. Weber, Nucl. Instrum. Methods Phys. Res. B **141**, 94 (1998).
[21]B. G. Svensson, C. Jagadish, A. Hallén, and J. Lalita, Phys. Rev. B **55**, 10498 (1997).
[22]*Zinc Oxide Bulk, Thin films and Nanostructures*, edited by C. Jagadish and S. J. Pearton (Elsevier, Oxford, 2006).
[23]P. Lèvègue, H. Kortegaard Nielsen, P. Pellegrino, A. Hallèn, B. G. Svensson, A. Yu. Kuznetsov, J. Wong-Leung, C. Jagadish, and V. Privitera, J. Appl. Phys. **93**, 871 (2003).
[24]F. A. Selim, M. H. Weber, D. Solodovnikov, and K. G. Lynn, Phys. Rev. Lett. **99**, 085502 (2007).